Poly(lactic acid) and Zeolite Composites Prepared by Melt Processing: Morphological and Physical–Mechanical Properties

Isinay E. Yuzay, Rafael Auras, Susan Selke

School of Packaging, Michigan State University, East Lansing, Michigan 48824

Received 15 May 2009; accepted 21 August 2009
DOI 10.1002/app.31322
Published online 7 October 2009 in Wiley InterScience (www.interscience.wiley.com).

ABSTRACT: Poly(lactic acid), PLA, composites containing 0, 1, 3, and 5 wt % zeolite type 4A were prepared using extrusion/injection compounding techniques. Morphological characterizations were carried out by scanning electron microscopy (SEM) and transmission electron microscopy (TEM). Physical properties were evaluated by differential scanning calorimetry (DSC) and dynamic mechanical analysis (DMA) and mechanical properties by standard tensile testing. The morphological studies showed a homogenous dispersion of zeolite particles within the PLA matrix. As the fracture stress propagated, zeolite particles remained embedded into the matrix, indicating the existence of good interfacial adhesion between zeolite particles and the PLA matrix. The improvement in the interfacial adhesion was also confirmed by applying Nicolais-Narkis and Pukanszky models. The percent crystallinity of the PLA and the temperature- dependant elastic and viscous modulus of the composite increased with the proportion of zeolites. © 2009 Wiley Periodicals, Inc. J Appl Polym Sci 115: 2262–2270, 2010

Key words: biopolymers; processing; mechanical properties; thermal properties; zeolites

INTRODUCTION

An increased awareness of environmental issues is driving the desire to use biodegradable and bio-based polymers. Poly(lactic acid), PLA, is one of the most widely used biodegradable/bio-based plastic alternatives to traditional petroleum-based plastics. PLA offers a range of potential advantages: it can be derived from renewable resources such as corn and sugar beets and can be composted under certain temperature and humidity conditions.[1,2] The production of PLA also requires less energy and produces less carbon dioxide than does that of traditional polymers.[3,4] Recently, several research efforts have been directed to develop PLA-based composites with high performance and/or functionality and extend PLA's current applications to new areas. The incorporation of various nano/microinorganic fillers has been shown to result in significant improvements in the properties of PLA.[1,3]

Zeolites are crystalline porous nanostructures with pore sizes ranging from about 3 to 15 Å. In general, the structure of zeolites consists of SiO_4 and AlO_4 tetrahedra, which form a network of channels and cavities. Extensive research has been done on natural and synthetic zeolites due to their intrinsic chemical reactivity, adsorptivity, and ion exchange capacity.[5,6] These features of the zeolites make their polymer composites multifunctional. For instance, sodium ions present in zeolites can be substituted by silver ions (Ag^+) and incorporation of silver ion-exchanged zeolites into the polymer matrix results in good antimicrobial properties.[7] Using various transition metal ions or dopants in zeolite pores also alters electrical conductivity properties of the polymer composites.[8,9] Zeolites are also being used in active packaging applications, particularly for fresh produce and vegetables which rapidly consume the oxygen in the package headspace, causing the deterioration of produce and vegetable quality.[7] Therefore, inclusion of zeolites into bio-based poly(lactic acid) holds promise for a wide range of polymer applications. In this study, an attempt has been made to develop an effective melt processing technique and evaluate the feasibility of using zeolite as a filler for PLA. To the best of the authors' knowledge, there is no data available on incorporation of zeolites into a PLA matrix, which could bring potential new packaging applications. Various polymers, such as poly(dimethylsiloxane), PDMS,[10] poly(ethersulfone), PES,[11] poly(imide),[12] poly(aniline), PANI,[13] low-density poly(ethylene), LDPE,[7] high-density poly(ethylene), HDPE,[14] poly(propylene), PP,[15] poly(vinyl alcohol), PVOH,[13] poly(vinyl acetate), PVAc,[16] ethylene vinyl acetate, EVAc,[17] poly(styrene), PS,[18] cellulose acetate, CA,[19] and poly(carbonate), PC,[20] have been used to

Correspondence to: S. Selke (sselke@msu.edu).
Contract grant sponsor: Center for Food and Pharmaceutical Packaging Research (CFPPR), Michigan State University.

produce zeolite composites mainly for gas and liquid separation purposes. In these studies, often a very large amount (up to 40–50 wt %) of zeolite was added to the polymer matrix. Most of the studies discussed the necessity of surface treatment of zeolites for better dispersion in the polymer matrix for improved properties.[21] Other studies argued that surface treatment may cause pore blockage, resulting in inferior gas and liquid separation.[22] Therefore, it is the purpose of this work to fabricate PLA composites containing a low amount of zeolites (0–5 wt %) in a twin-screw extruder, thus facilitating dispersion and to evaluate the effect of zeolites on the physical, mechanical, and thermal properties of the PLA composites.

EXPERIMENTAL

Materials

Poly(lactic acid) resin produced from 94% L-lactide were obtained from NatureWorks LLC (Blair, NE). Synthetic zeolite (type 4A) (Si/Al:1) with a pore size of 3.8–4 Å was supplied by UOP LLC, (Des Plaines, IL) in the form of powder. An SEM micrograph of type 4A zeolite particles with an average particle size of 1–2 μm is shown in Figure 1. Before processing, PLA resin pellets and zeolite powders were dried in a vacuum oven at 60°C for 4 h and at 100°C for 24 h, respectively.

Preparation of composites

PLA composites containing 0 to 5 wt % zeolite type 4A were prepared using a microextruder (DSM Research, The Netherlands) equipped with corotating twin-screws having lengths of 150 mm, *L/D* ratio of 18, and capacity of 15 cc. The extrusion was carried out at 185°C for 5 min at a screw rotation speed of 100 rpm for both PLA and PLA/zeolite composites. After the set extrusion time, the extrudates were collected from the die and transferred into a mini-injection molder (DSM Research, The Netherlands) by a preheated transfer cylinder to prepare test specimens for physical and mechanical property evaluation. The optimized injection pressure was 896 kPa, and the mold temperature was kept at 30°C. Test specimens were wrapped in aluminum foil and stored at 23°C and 50% relative humidity before testing.

Characterization of composites

Microscopy

Scanning electron microscopy (SEM). Morphological analyses were done using a SEM JSM 6400 (JOEL, Tokyo, Japan) equipped with a LaB_6 emitter. The fractured surfaces of PLA and PLA/zeolite composites were sputter coated with ~ 15 nm of gold and SEM micrographs were collected at an accelerating voltage of 15 kV using various magnifications.

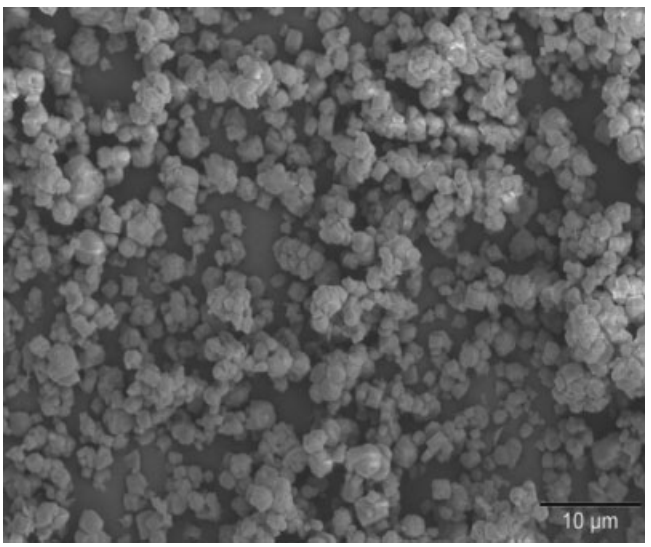

Figure 1 SEM micrograph of zeolite type 4A particles. Magnification: ×5000; Scale bar: 10 μm.

Transmission electron microscopy (TEM). TEM bright field images were taken using a JOEL 100CX (JOEL, Tokyo, Japan) operated at an accelerating voltage of 150 kV. PLA/zeolite composite samples (the middle part of tensile dumbbell specimens) were ultramicrotomed with a diamond knife to give ~ 70-nm thick sections, and then, the sections floating on the distilled water were transferred to carbon-coated copper grids of 300 mesh.

Tensile properties

Dumbbell-shaped specimens obtained by injection molding were used for the tensile tests. Tensile properties such as tensile strength, modulus of elasticity, and elongation at break, of PLA/zeolite composites containing 0, 1, 3, and 5 wt % zeolite were measured in accordance with ASTM D 638-03[23] using an Instron Model 5565 tensile tester (Instron Corp., Canton, MA) with a load cell of 5 kN. The initial grip distance was 50 mm and the crosshead speed was 50 mm/min. Five specimens were tested for each composite and the mean values and standard deviation are reported.

Dynamic mechanical analysis

The temperature dependence of storage modulus (E'), loss modulus (E''), and damping factor (tan delta) of PLA/zeolite composites was evaluated using a DMA Q800 (TA Instruments, NewCastle, DE). The test was carried out by heating the samples at a rate of 2°C/min from room temperature to

90°C. The samples were tested in a dual cantilever mode at an oscillating amplitude of 15 μm and a frequency of 1 Hz. A minimum of three injection molded specimens with dimensions of 58 mm × 12 mm × 2 mm (length × width × thickness) were tested for each composite combination.

The heat deflection temperature (HDT) of PLA/zeolite composites was also measured by a DMA Q800 (TA Instruments, NewCastle, DE) operating in three-point bending mode according to ASTM D648-03.[24] The specimens were heated at a rate of 2°C/min from room temperature to 80°C under a constant load of 0.455 MPa, and the HDT was determined as the temperature at which the specimens reached 0.2% strain. Three test specimens with dimensions of 58 mm × 12 mm × 2 mm were tested for each composite combination.

Differential scanning calorimetry

The thermal analyses of PLA/zeolite composites were performed on a differential scanning calorimeter (DSC) Q100 (TA Instruments, NewCastle, DE) in accordance with ASTM D3418-03.[25] Approximately 5–8 mg of injection molded samples were heated from room temperature to 190°C at a rate of 10°C/min under a constant nitrogen flow (70 mL/min). For each sample, the glass transition temperature (T_g), cold-crystallization temperature (T_{cc}), melting temperature (T_m), and enthalpies of cold crystallization (ΔH_{cc}), and melting (ΔH_m) were evaluated from the DSC thermograms. The degree of crystallinity (X_c) of PLA and PLA/zeolite composites was calculated based on the following equation:

$$X_c(\%) = [(\Delta H_m - \Delta H_{cc})/(\Delta H_f(1-x))] \times 100 \quad (1)$$

where ΔH_f is the enthalpy of fusion of an 100% crystalline PLA which is 93.7 J/g,[2,26] and x is the weight fraction of zeolite in the composite. At least five specimens were tested for each composite combination.

Statistical analysis

Results are reported as mean ± standard deviation. Data were evaluated by analysis of variance (ANOVA)—Tukey using the software InfoStat Ver1.0 (Estadistica y Biometria-Universidad Nacional Cordoba). Significance was defined as $P < 0.05$.

RESULTS AND DISCUSSION

Morphology

The fracture surfaces of PLA and PLA/zeolite composites were examined using SEM and TEM to evaluate the size, shape, and dispersion of zeolites in the PLA matrix. Zeolite type 4A particles exhibited a cubical

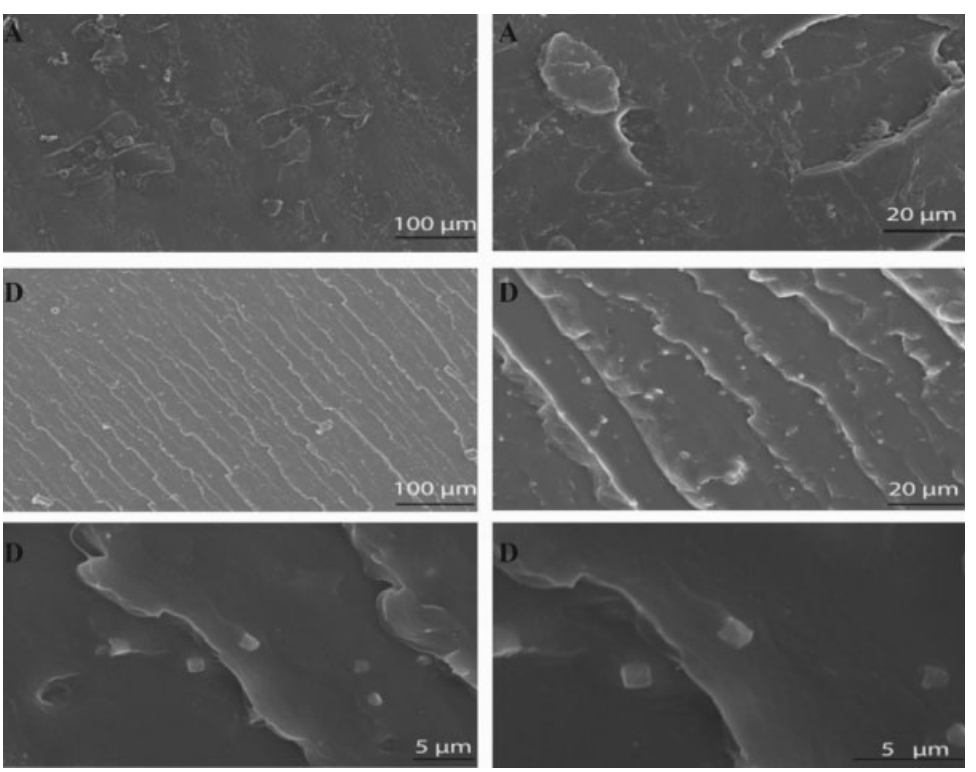

Figure 2 SEM micrographs of neat PLA and PLA/zeolite composites. (A) PLA neat-200 (scale bar = 100 μm) and 1000 (scale bar = 20 μm) magnification, (D) PLA with 5 wt % zeolite- 200 (scale bar = 100 μm), 1000 (scale bar = 20 μm), 3300 (scale bar = 5 μm), and 6000 (scale bar = 5 μm) magnification.

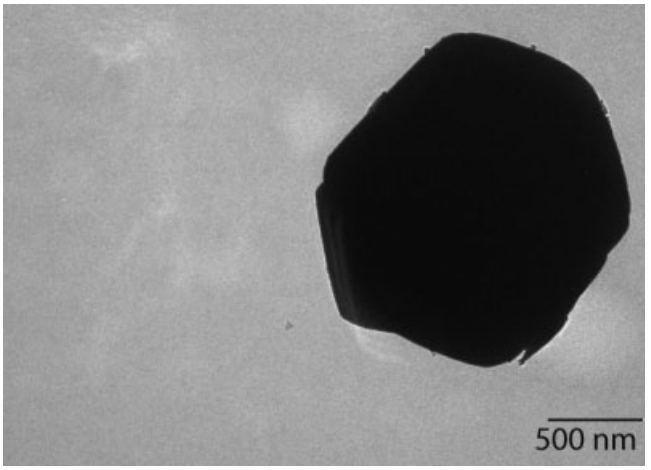

Figure 3 TEM image of individual zeolite crystal. Magnification: ×40,000; Scale bar: 500 nm.

shape with an average particle size ranging from 0.7 to 2 μm (Figs. 2 and 3). Good particle dispersion in the PLA matrix was visually observed. As the fracture stress propagated in the composites, zeolite particles remained embedded into the PLA matrix. At lower magnifications, neither void formation around the zeolite particles nor cavities in the PLA matrix were observed, indicating the existence of good interfacial adhesion between zeolite type 4A particles and the PLA matrix (Figs. 2 and 3). Mahajan and Koros[27] also observed similar improved adhesion between PVAc and zeolite type 4A mixed matrix membranes. The good contact between PVAc and zeolite type 4A was attributed to the affinity of PVAc for alumina, the flexibility of the polymer during membrane formation, and molecular adsorption of the polymer onto the zeolite surface. However, other attempts[12,22] at developing mixed matrix membranes, which combined glassy polymers such as polyimide and PES with zeolite type 4A, resulted in extremely poor interfacial adhesion between zeolite and polymer matrices. This was mainly attributed to weak interaction between zeolite and polymer matrices, having a very rigid nature of the polymers (T_g values varied from 200 to 305°C), and uneven shrinkages and stresses generated during the solvent removal after casting the membranes.[28] Using PLA as a polymer matrix, whose T_g value is around 60°C, and melt compounding the PLA /zeolite composites helped us to obtain good interfacial adhesion. This good interfacial adhesion may also be due to dipolar interaction or hydrogen bonding between PLA and zeolite type 4A.

Tensile properties

Table I presents a comparison of tensile properties of PLA and PLA/zeolite composites with different zeolite loadings. It can be seen that the addition of zeolite type 4A particles increased the tensile strength and modulus of elasticity, while decreasing the elongation at break. The tensile strength of PLA/zeolite composites slightly increased with the addition of 3 wt % zeolite; however, the inclusion of 3 wt % zeolite increased the modulus of elasticity by 20%. With further addition of zeolite (i.e., 5 wt %), the value of the modulus of elasticity leveled off. This amount might be the threshold for the formation of agglomerates. Adding 5 wt % zeolite decreased the elongation at break for the PLA from 10.96 ± 2.3 to 6.60 ± 0.8%. In general, the addition of rigid particulate fillers increases the tensile modulus, but drastically reduces the elongation at break. In many cases, filler particles also decrease the tensile strength of the polymer matrix, but there are some exceptions. In these cases, the tensile strength may increase due to good adhesion between filler and matrix.[29,30] It is clear that the interfacial adhesion between the zeolites and the PLA matrix and the dispersion of zeolite particles in the PLA matrix was good enough to maintain the tensile strength. Metin et al.[31] and Sun et al.[32] reported a decrease in tensile strength when combining PP with natural zeolite, and chitosan with H-ZSM-5, synthetic zeolite Si/Al ratio of 25, respectively. The investigators tried to overcome the reduction in the tensile strength of PP and chitosan matrices by using several silane coupling agents, improving the filler-polymer adhesion at the interface.

A number of theories and empirical models have been developed to evaluate the mechanical and interfacial properties of polymers filled with particulate fillers. Such models usually assume either that there is no interaction between the filler and the matrix or that there is good adhesion between the filler and the matrix. Since the nature of interactions between zeolite and PLA matrix is yet not clear, we considered all assumptions as plausible scenarios of PLA/zeolite composites while using individual models to predict the tensile strength of PLA/zeolite

TABLE I
The Effect of Zeolite Content on Tensile Properties of PLA[N1,N2]

Zeolite loadings (wt %)	Tensile strength (MPa)	Elongation at break (%)	Modulus of elasticity (MPa)
0	62.2 ± 5.4[a]	10.9 ± 2.3[b]	1221 ± 64.5[a]
1	62.5 ± 3.2[a]	6.9 ± 2.0[a]	1295 ± 127.1[a]
3	67.9 ± 1.4[b]	6.9 ± 0.2[a]	1465 ± 147.5[b]
5	64.2 ± 3.4[a b]	6.6 ± 0.8[a]	1465 ± 56.1[b]

[N1] Mean ± standard deviation.
[N2] Means with different superscript letters in the same columns are significantly different ($P < 0.05$).

composites. Although cubical zeolite particles were introduced into the PLA matrix, the models developed for spherical particles were used to predict the mechanical properties. It was assumed that the models developed for the spherical fillers would be applicable to zeolite particles since cubical particles have the same dimension in all directions.

The Nicolais-Narkis model[33] and its modifications are the most widely used models to predict the effects of interfacial interaction on tensile yield strength for the case of poor adhesion between the spherical filler particle and the polymer matrix. In the Nicolais-Narkis model, the tensile strength values of the composite can be predicted by the following equation:

$$\sigma_c = \sigma_m(1 - KV_f^{2/3}) \quad (2)$$

where σ_c and σ_m are the tensile strength of the composite and matrix, respectively, and V_f is the volume fraction of filler. K is a parameter expressing the filler-matrix interaction. According to this model, the value of K becomes 1.21 in the absence of adhesion between the filler and the matrix which means the load is sustained only by the polymer matrix and addition of fillers leads to reduction in the tensile strength of the composite.[34,35] If the value of K is less than 1.21, the tensile strength of the composite increases which is evidence of improved adhesion between the filler and the matrix.

In the case of strong filler-matrix interfacial adhesion, a simple model developed by Pukanszky et al.[36,37] to predict the tensile strength of the polymer composites can be expressed by the following equation:

$$\frac{\sigma_c}{\sigma_m} = \frac{1 - V_f}{1 + 2.5V_f}\exp(BV_f) \quad (3)$$

where σ_c and σ_m are the tensile yield stress of the composite and the matrix, respectively, V_f is the volume fraction of the filler, and B is an interaction parameter, which depends on the surface area of the fillers, the thickness of the interface, filler density, and interfacial bonding energy. The pre-exponential term in eq. (3) is related to the decrease of the effective load-bearing cross section of the matrix while the exponential term, $\exp(BV_f)$, describes the interfacial interactions in the composite.[34,38,39] Equation (3) can be rearranged in a linear form. Ln $[(\sigma_c(1 + 2.5V_f)/(\sigma_m(1 - V_f)]$ is plotted as a function of V_f and then the interaction parameter, B, can be calculated from the slope of the straight line. In general, if the value of B is zero, the filler acts as a void. The higher B value indicates stronger interfacial interactions between the filler and the matrix. It was shown in the Refs. [31,40,41] that if the value of B is more than 3, the filler-matrix interface is considered strong and a reinforcing effect of filler can be obtained.

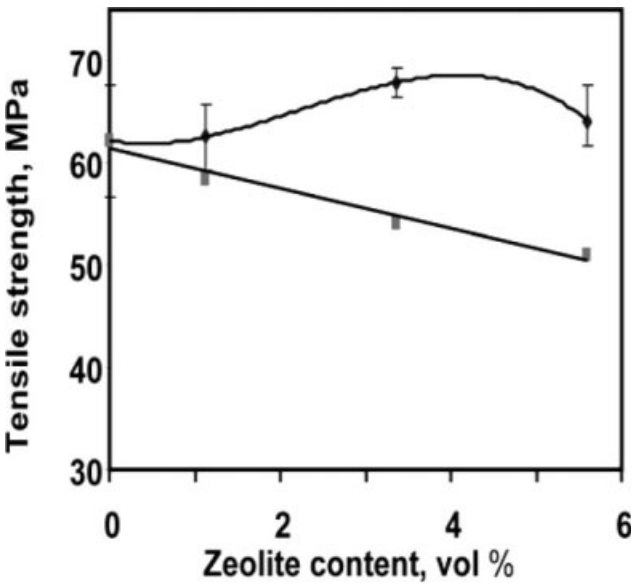

Figure 4 Comparison of experimental tensile strength data with the Nicolais-Narkis model for PLA/zeolite composites. Experimental tensile strength data (●) and Nicolais-Narkis predicted data (■) with the adhesion K value of 1.21.

In this study, both the Nicolais-Narkis and Pukanszky equations were applied to the tensile stress data of PLA/zeolite composites to evaluate the interfacial interaction between the zeolites and the PLA matrix. It can be seen from Figure 4 that the Nicolais-Narkis model based on the hypothesis of zero adhesion between the zeolite and the PLA matrix predicted a decrease in tensile strength that was not observed, which is evidence of the interfacial adhesion between zeolite particles and the PLA matrix.

The Pukanszky model was also applied to experimental tensile data under the assumption that good bonding exists between the zeolites and the PLA matrix. The plot of Ln $[(\sigma_c(1+2.5V_f)/(\sigma_m(1 - V_f)]$ as function of V_f is shown in Figure 5. The average B values calculated from the slopes of the straight lines for each zeolite volume fraction are also indicated on Figure 5. All of the average B values were higher than 3 which confirms the presence of interfacial interactions between the zeolite particles and the PLA matrix. The composites containing 3 wt % zeolite exhibited the highest B value, 6.0, implying the strongest interfacial interaction compared with PLA/zeolite 1 wt % and PLA/zeolite 5 wt % composites. This prediction agrees with the slightly higher tensile strength measure of PLA/zeolite 3 wt % shown in Table I. Increasing the filler content from 3 to 5 wt % led to a reduction in the B value, yet still the B value was higher than 3, which might prevent

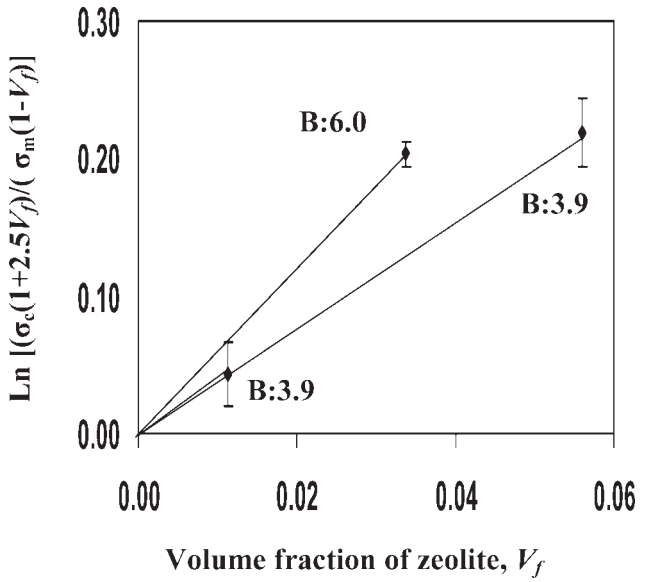

Figure 5 The tensile stress of PLA/zeolite composites in the linear form of Eq. (3). The average interaction parameters (B) determined from the slopes of the straight lines. Note: The 95% confidence interval of the mean B values are 5.7, 0.7, and 1.1 at the zeolite volume fractions of 0.01126(1 wt %), 0.03369(3 wt %), and 0.05601(5 wt %), respectively.

the occurrence of debonding at the zeolite-PLA interface. The comparison of the experimental data with the Pukanszky model is also shown in Figure 6. The experimental data points remain between the straight lines obtained from the Pukansky equation using the B values of 3.0 and 6.0. In the study of Metin et al.[31], PP composites containing untreated and treated natural zeolites were evaluated in terms of interfacial adhesion. PP with untreated natural zeolite composites exhibited a B value of minus 9. Treatment of the natural zeolites with an amino functional silane coupling agent increased the B value to 2.15 which was considered an indication of strong interaction. Similar results were also reported by Demjen et al.[42] for PP/$CaCO_3$ composites. Thus, the B values obtained from this study without using any coupling agents indicated good interfacial interactions between the zeolite particles and the PLA matrix.

Dynamic mechanical thermal analysis

Figure 7(A) shows the storage and loss modulus of PLA and PLA zeolite composites at various zeolite loadings. The storage modulus denotes the maximum energy stored in the material during straining [the oscillation cycle or cycle of sinusoidal deformation]. When the applied mechanical energy is not stored, it is converted into heat via molecular friction. Therefore, this energy dissipated as heat is called the loss modulus. As can be seen in Figure 7(A), the storage modulus of PLA/zeolite composites was higher than that of the neat PLA matrix. Addition of 5 wt % zeolite type 4A increased the storage modulus of PLA from 3100 to 3854 MPa at 30°C; however, the storage modulus was not affected by low zeolite content (i.e., 1 wt %) at room temperature. When the PLA was heated through the glass transition region, zeolites had more pronounced effects on the storage modulus. In the vicinity of 60°C, the storage modulus of PLA with 5 and 3 wt % zeolites dropped abruptly while the storage modulus of neat PLA exhibited a sudden decrease at about 49°C. As can be seen, the stiffening effect of the zeolites was significant at higher temperatures. The increase in storage modulus with increasing zeolite content means that the stress was transferred from the matrix to the zeolite particles that introduced stiffness into the matrix. Similar behavior was reported by other researchers using fibers, talc, and clays.[43,44] The loss modulus values also increased with zeolite loading. The loss modulus of PLA and PLA with 5 wt % zeolite composites reached a maximum value of 668 MPa at 59.0°C and 901 MPa at 60.6°C, respectively. These results show that PLA/zeolite composites have better ability to dissipate the vibrational energy as heat than does the neat PLA.

Figure 7(B) exhibits the tan delta temperature curves for PLA and PLA/zeolite composites. The tan delta denotes material damping characteristics. It is mainly a measurement of the ratio of loss modulus to storage modulus. The tan delta peak of the PLA with 5 wt % zeolite composite shifted to a

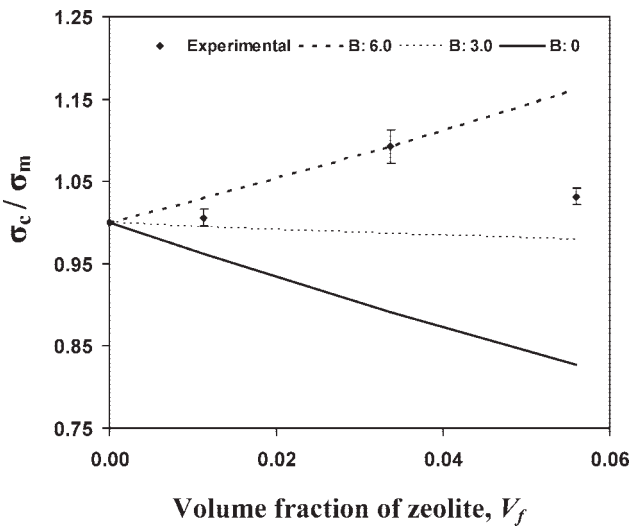

Figure 6 Experimental and predicted relative tensile yield stress (σ_c/σ_m) of PLA composites as a function of zeolite volume fraction: ● Experimental data; straight line according to the Pukanszky equation with B : 0; dotted and dashed lines according to the Pukanszky equation with B : 3.0 and 6.0, respectively.

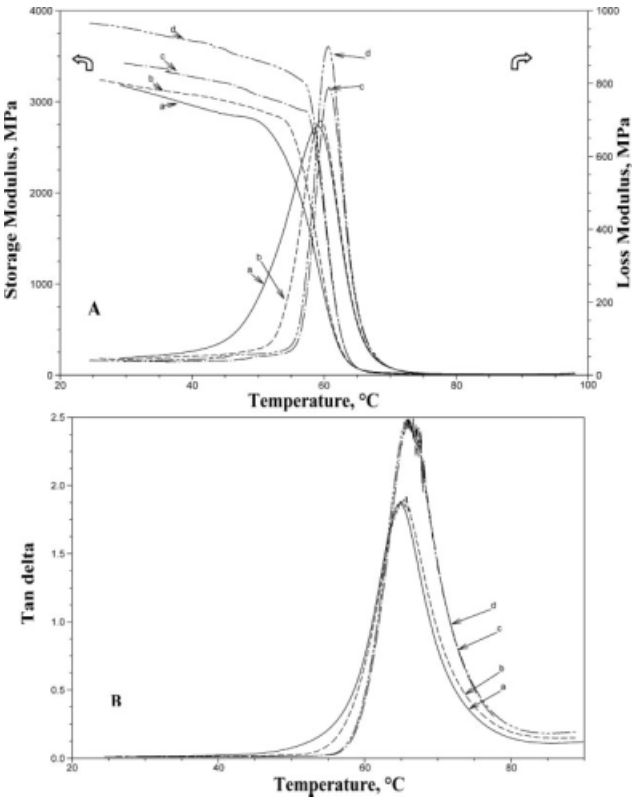

Figure 7 Storage modulus (A), loss modulus (A), and tan delta (B) of PLA and PLA/zeolite composites as a function of temperature.(a: — PLA); (b: —— — PLA with 1 wt % zeolite); (c: —•— PLA with 3 wt % zeolite); (d: —••— PLA with 5 wt % zeolite).

slightly higher temperature. Additionally, the intensity of the tan delta peak was increased in comparison with the neat PLA. This high magnitude of tan delta may suggest that the PLA with 5 wt % zeolite composites has better damping properties than the neat PLA. Nielsen and Landel suggest[29] that the effects of rigid fillers on the damping of polymers can be estimated by the following equations:

$$\left(\frac{E''}{E'}\right)_{\text{comp}} = \tan\text{delta}_{\text{comp}} = (\tan\text{delta}_{\text{matrix}} \times \varphi_{\text{mattrix}}) + (\tan\text{delta}_{\text{filler}} \times \varphi_{\text{filler}}) \quad (4)$$

$$\left(\frac{E''}{E'}\right)_{\text{comp}} = \tan\text{delta}_{\text{comp}} = \tan\text{delta}_{\text{matrix}} \times (1 - \varphi_{\text{filler}}) \quad (5)$$

where E'' and E' are the loss and storage modulus, respectively, and φ_{matrix} and φ_{filler} are the volume fractions of matrix and filler, respectively. Since the damping of most rigid fillers is very low compared to the damping to the polymers, the second term in eq. (4) can be neglected. Therefore, eq. (4) can be rewritten as eq. (5). This equation suggests that the incorporation of fillers decreases the peaks of energy dissipation curves due to the decrease in volume fraction of the matrix. In the literature, there are several studies showing a decrease in tan delta values after inclusion of fillers.[43,45] In our study, the effect of the zeolites on the dissipation energy was an exception; the zeolite increased the damping properties. Nielsen and Landel[29] suggest that the increased damping may result from induced thermal stresses or changes in polymer conformation or morphology.

The heat deflection temperature (HDT) of neat PLA was found to be 55.1°C ± 0.1°C. The 3-point bending test showed that the HDT value of PLA was not much affected by the presence of zeolite (Table II). This implied that either the amount of zeolite was not sufficient to improve the HDT or that zeolites are incapable of raising the HDT. The HDT might be improved by raising the degree of crystallinity, glass and melting temperatures, or combination of all. While the percent crystallinity of PLA increased from 3.2 ± 0.7 to 7.6 ± 1.2 with 5 wt % zeolite, this small increase did not result in any change in the HDT value.

Thermal analysis

The thermal characteristics of PLA and PLA/zeolite composites were evaluated using a DSC. The transition temperatures along with the calculated percentages of crystallinity of PLA and PLA/zeolite composites are summarized in Table III. The zeolite type 4A content did not affect the glass transition and melting temperature of the PLA matrix; however, the cold crystallization and percent crystallinity were affected. PLA and PLA/zeolite composites exhibited not only well-defined T_g values at around 58°C but also endothermic peaks immediately after the glass transition temperatures. These endothermic peaks represent excess enthalpy relaxation resulting from the thermal and mechanical history of PLA and PLA/zeolite composites prepared by extrusion followed by injection molding. The representative DSC heat flow curves for the unprocessed PLA (PLA pellets), PLA, and PLA with 5 wt % zeolite

TABLE II
The Heat Deflection Temperature (HDT) of PLA/Zeolite Composites[N1, N2]

Zeolite content (wt %)	HDT (°C)
0	55.1 ± 0.1[a,b]
1	55.5 ± 0.5[b]
3	54.2 ± 0.5[a]
5	54.4 ± 0.3[a]

[N1] Mean ± standard deviation.
[N2] Means with different superscript letters in the same columns are significantly different ($P < 0.05$).

TABLE III
Thermal Characteristics of PLA and PLA/Zeolite Composites[N1,N2]

Zeolite content wt %	T_g (°C)	T_{cc}(°C)	T_m (°C)		X_c (%)
			T_{m1}	T_{m2}	
0[a]	56.4 ± 0.9[b]	-	-	158.6 ± 1.0[c]	37.3 ± 1.6[d]
0	58.5 ± 0.7[e]	123.6 ± 4.0[f]	148.0 ± 3.7[e]	153.8 ± 0.7[e]	3.2 ± 0.7[e]
1	57.9 ± 1.7[e]	119.0 ± 1.2[c]	149.9 ± 0.8[e]	153.9 ± 1.1[e]	5.2 ± 1.1[c e]
3	57.5 ±1.5[e]	116.7 ± 3.4[c e]	149.1 ± 1.6[e]	154.7 ± 2.2[e]	6.2 ± 2.2[c f]
5	58.7 ±1.7[e]	114.3 ± 1.6[e]	148.0 ± 1.4[e]	155.0 ± 1.2[e]	7.6 ± 1.2[f]

[a] PLA pellet (unprocessed PLA).
[b] Week and broad heat increment.
[N1] Mean ± standard deviation.
[N2] Means with different superscript letters (c–f) in the same columns are significantly different ($P < 0.05$).

composites are shown in Figure 8. As expected, there was no endothermic peak following the T_g for the unprocessed PLA due to lack of thermal and mechanical history. In addition, a weak and broad glass transition appeared for the PLA pellets. The deflection point at the base line was difficult to observe. This could be attributed to a high degree of crystallinity of the pellets. The mobility of the molecules in the amorphous region could be confined by the presence of the crystalline regions, which makes the T_g difficult to detect.[46] The endothermic peaks at around 58°C for PLA and PLA with 5 wt % zeolite were clearly evident in the thermograms.

Upon heating from room temperature, the PLA molecular chains gained mobility after the glass transition and then began formation of crystallites in the region of the cold-crystallization exotherm. As can be seen from Table III, all of the injection molded samples, excluding PLA pellets, underwent cold crystallization at the heating rate of 10°C/min. In general, a low-cold-crystallization temperature is considered as an indirect indication of fast crystallization. With the addition of 5 wt % zeolite, the cold-crystallization-temperature of PLA shifted from 123.6°C ± 4.0°C to 114.3°C ± 1.6°C. This reduction in the cold-crystallization-temperature suggests a nucleating effect of the zeolite particles. A similar nucleating effect of zeolites in PP crystallization has been reported by Pehlivan et al.[47] In a study of mesoporous zeolites (MCM-41), Run et al.[48] prepared PET/mesoporous zeolite composites using *in situ* polymerization and observed that the inclusion of mesoporous zeolites acted as nucleating agents in the PET matrix.

Another interesting phenomenon is the bimodal (double peak) melting endotherms of PLA and PLA/zeolite composites. Although the unprocessed PLA exhibited only one melting endotherm at 158.6°C ± 1.0°C, the injection molded PLA samples showed the main melting peaks at 148.0°C ± 3.7°C and an additional peak (small shoulder) at 153.8°C ± 0.7°C. Several researchers have observed similar bimodal melting behavior for PLA and its composites.[49–52] These peaks were attributed to the existence of different crystalline structures (i.e., variation in thickness of the lamellas and size of spherulites) being formed during heating and cooling in the DSC scans or processing.[52–54] The lower temperature peak, T_{m1}, usually corresponds to β crystals and the upper temperature peak, T_{m2}, corresponds to α crystals of PLA as established in the Refs. [52,55,56]. In the case of PLA–filler composites, the inclusion of fillers might also accelerate the growth of additional crystalline forms by creating defects in the structure.[46]

As can be seen from Table III and Figure 8, there were no significant changes in these melting temperatures with the addition of zeolites into the PLA

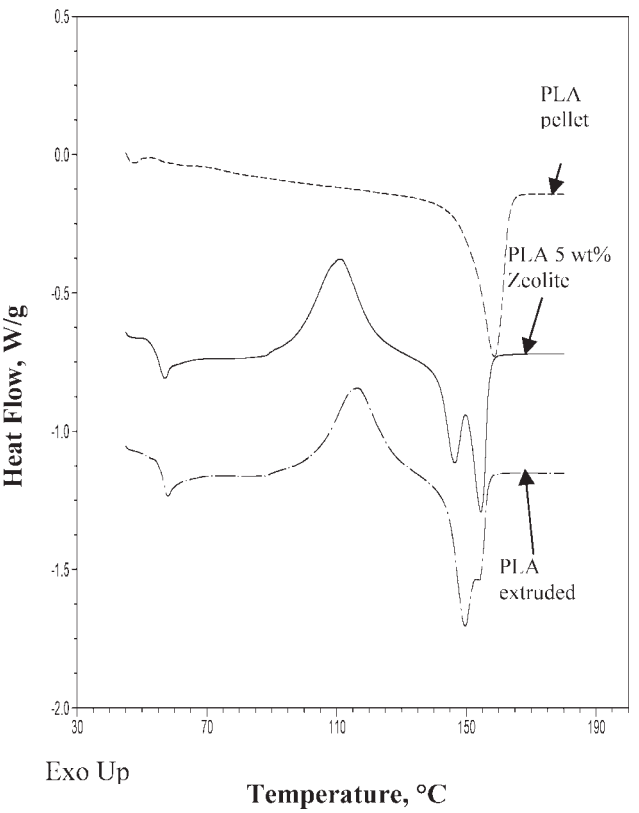

Figure 8 Representative DSC thermograms of PLA pellet, PLA extruded, and PLA with 5 wt % zeolite composites (Heating Ramp: 10°C/min).

matrix; however, the double melting peaks were more pronounced upon increasing the zeolite content. The percent crystallinity of PLA pellets and injection molded PLA samples were found to be 37.3% ± 1.6% and 3.2% ± 0.7%, respectively. This result suggests that injection molded test specimens were nearly amorphous and the percent crystallinity of injection molded PLA significantly increased with the amount of zeolite.

CONCLUSIONS

PLA/zeolite composites were successfully fabricated using extrusion followed by injection molding processes. The morphological studies showed a homogenous dispersion of zeolite type 4A in the PLA matrix. As the stress propagated through the composites, zeolite particles remained embedded into the matrix, indicating the existence of good interfacial adhesion between zeolite particles and the PLA matrix. The percent crystallinity of the PLA increased with the proportion of zeolites while no significant changes occurred in the glass transition, melting, and heat deflection temperature. With addition of 5 wt % zeolite, the storage modulus, loss modulus, and damping were enhanced. The modulus of elasticity was also positively correlated with zeolite content while the elongation at break was reduced with increasing zeolite loading.

References

1. Auras, R.; Harte, B.; Selke, S. Macromol Biosci 2004, 4, 835.
2. Auras, R.; Harte, B.; Selke, S. J Appl Polym Sci 2004, 92, 1790.
3. Sinha Ray, S.; Bousmina, M. Prog Mater Sci 2005, 50, 962.
4. Murariu, M.; Da Silva Ferreira, A.; Degee, P.; Alexandre, M.; Dubois, P. Polymer 2007, 48, 2613.
5. Barrer, R. M. Zeolites and Clay Minerals as Sorbents and Molecular Sieves; Academic Press: London, 1978.
6. Yang, R. T. Adsorbents: Fundamentals and Applications; Wiley: Hoboken, NJ, 2003.
7. Brody, A.; Strupinsky, E.; Kline, L. Active Packaging for Food Applications; Technomic Publishing Co: Lancaster, PA, 2001.
8. Chuapradit, C.; Wannatong, L. R.; Chotpattananont, D.; Hiamtup, P.; Sirivat, A.; Schwank, J. Polymer 2005, 46, 947.
9. Vitoratos, E.; Sakkopoulos, S.; Dalas, E.; Malkaj, P.; Anestis, C. Curr Appl Phys 2007, 7, 578.
10. Clarizia, G.; Algieri, C.; Drioli, E. Polymer 2004, 45, 5671.
11. Huang, Z..; Li, Y.; Wen, R.; Teoh, M. M.; Kulprathipanja, S. J Appl Polym Sci 2006, 101, 3800.
12. Pechar, T. W.; Kim, S.; Vaughan, B.; Marand, E.; Tsapatsis, M.; Jeong, H. K. J Membr Sci 2006, 277, 195.
13. Naidu, B. V. K.; Bhat, S. D.; Sairam, M.; Wali, A. C.; Sawant, D. P.; Aminabhavi, T. M. J Appl Polym Sci 2005, 96, 1968.
14. Kim, H.; Biswas, J.; Choe, S. Polymer 2006, 47, 3981.
15. Ozmihci, F.; Balkose, D.; Ulku, S. J Appl Polym Sci 2001, 82, 2913.
16. Moore, T. T.; Vo, T.; Mahajan, R.; Kulkarni, S.; Hasse, D.; Koros, W. J. J Appl Polym Sci 2003, 90, 1574.
17. Yan, Y.; Zhao, Y.; Liu, M. J Appl Polym Sci 2005, 96, 1460.
18. Sales, M. J. A.; Dias, S. C. L.; Dias, J. A.; Pimentel, T. A. Polym Degrad Stab 2005, 87, 153.
19. Duval, J. M.; Kemperman, A. J. B.; Folkers, B.; Mulder, M. H. V.; Desgrandchamps, G.; Smolders, C. A. J Appl Polym Sci 1994, 54, 409.
20. Sen, D.; Kalipcilar, H.; Yilmaz, L. J Membr Sci 2007, 303, 194.
21. Mahajan, R.; Koros, W. J. Polym Eng Sci 2002, 42, 1432.
22. Moore, T. T.; Koros, W. J. J Mol Struct 2005, 739, 87.
23. American Society for Testing and Materials. In Annual Book of ASTM Standards; ASTM: Philadelpia, PA, 2004; 8:01, D 638–03.
24. American Society for Testing and Materials. In Annual Book of ASTM Standards; ASTM: Philadelpia, PA, 2004; 8:01, D 648–03.
25. American Society for Testing and Materials. In Annual Book of ASTM Standards; ASTM: Philadelpia, PA, 2004; 8:02, D 3418–03.
26. Sinha Ray, S.; Yamada, K.; Okamoto, M.; Ogami, A.; Ueda, K. Chem Mater 2003, 15, 1456.
27. Mahajan, R.; Koros, W. J. Ind Eng Chem Res 2000, 39, 2692.
28. Li, Y.; Guan, H.; Chung, T.; Kulprathipanja, S. J Membr Sci 2006, 275, 17.
29. Nielsen, L. E.; Landel, R. F. Mechanical Properties of Polymers and Composites; Marcel Dekker: New York, 1994.
30. Sekutowski, D. In Plastics Additives and Modifiers Handbook; Edenbaum, J., Ed.; Van Norstrand Reinhold: New York, 1992.
31. Metin, D.; Tihminlioglu, F.; Balkose, D.; Ulku, S. Compos Part A Appl Sci Manuf 2004, 35, 23.
32. Sun, H.; Lu, L.; Chen, X.; Jiang, Z.. Appl Surf Sci 2008, 254, 5367.
33. Nicolais, L.; Narkis, M. Polym Eng Sci 1971, 11, 194.
34. Fu, S.-Y.; Feng, X.-Q.; Lauke, B.; Mai, Y.-W. Compos Part B Eng 2008, 39, 933.
35. Willett, J. L.; Felker, F. C. Polymer 2005, 46, 3035.
36. Turcsanyi, B.; Pukanszky, B.; Tudos, F. J Mater Sci Lett 1988, 7, 160.
37. Pukanszky, B.; Turcsanyi, B.; Tudos, F. Interfaces in Polymer, Ceramic and Metal Matrix Composites; Ishida, H., Ed.; Elsevier: Amsterdam, 1988; p 467–477.
38. Danyadi, L.; Renner, K.; Moczo, J.; Pukanszky, B. Polym Eng Sci 2007, 47, 1246.
39. Kiss, A.; Fekete, E.; Pukánszky, B. Compos Sci Technol 2007, 67, 1574.
40. Kaully, T.; Siegmann, A.; Shacham, D. Polym Compos 2008, 29, 396.
41. Papanicolaou, G. C.; Xepapadaki, A. G.; Kotrotsos, A.; Mouzakis, D. E. J Appl Polym Sci 2008, 109, 1150.
42. Demjen, Z.; Pukanszky, B.; Nagy, J. Compos Part A Appl Sci Manuf 1998, 29, 323.
43. Huda, M. S.; Drzal, L. T.; Mohanty, A. K.; Misra, M. Compos Part B Eng 2007, 38, 367.
44. Joseph, P. V.; Mathew, G.; Joseph, K.; Groeninckx, G.; Thomas, S. Compos Part A Appl Sci Manuf 2003, 34, 275.
45. Lu, J.; Wang, T.; Drzal, L. T. Compos Part A Appl Sci Manuf 2008, 39, 738.
46. Hatakeyama, T.; Quinn, F. X. Thermal Analysis: Fundamentals and Applications to Polymer Science; Wiley: Chichester, England, 1999.
47. Pehlivan, H.; Balkose, D.; Ulku, S.; Tihminlioglu, F. Compos Sci Technol 2005, 65, 2049.
48. Run, M.; Wu, S.; Zhang, D.; Wu, G. Polymer 2005, 46, 5308.
49. Shieh, Y. T.; Liu, G. L. J Polym Sci Part B: Polym Phys 2007, 45, 1870.
50. Sanchez-Garcia, M. D.; Gimenez, E.; Lagaron, J. M. Carbohydr Polym 2008, 71, 235.
51. Chen, G.-X.; Shimizu, H. Polymer 2008, 49, 943.
52. Jacobsen, S.; Fritz, H. G.; Degée, P.; Dubois, P.; Jérôme, R. Polymer 2000, 41, 3395.
53. Yasuniwa, M.; Tsubakihara, S.; Sugimoto, Y.; Nakafuku, C. J Polym Sci Part B: Polym Phys 2004, 42, 25.
54. Wang, Y.; Mano, J. F. Eur Polym J 2005, 41, 2335.
55. Pan, P.; Zhou, B.; Kai, W.; Dong, T.; Inoue, Y. J Appl Polym Sci 2008, 107, 54.
56. Dilorenzo, M. L. Macromol Symp 2006, 234, 176.